Pharmacokinetics of a novel anticancer ruthenium complex (KP1019, FFC14A) in a phase I dose-escalation study

Frederike Lentz[a], Anne Drescher[a], Andreas Lindauer[a], Magdalena Henke[b], Ralf A. Hilger[b], Christian G. Hartinger[c], Max E. Scheulen[b], Christian Dittrich[d], Bernhard K. Keppler[c] and Ulrich Jaehde[a] in collaboration with Central European Society for Anticancer Drug Research-EWIV

A phase I and pharmacokinetic study was carried out with the new ruthenium complex indazolium trans-[tetrachlorobis(1H-indazole)ruthenate(III)] (KP1019, FFC14A). Seven patients with various types of solid tumours refractory to standard therapy were treated with escalating doses of KP1019 (25–600 mg) twice weekly for 3 weeks. No dose-limiting toxicity occurred. Ruthenium plasma concentration–time profiles after the first dose and under multiple-dose conditions were analysed using a compartmental approach. The pharmacokinetic disposition was characterised by a small volume of distribution, low clearance and long half-life. Only a small fraction of ruthenium was excreted renally. The area under the curve values increased proportionally with dose indicating linear pharmacokinetics. *Anti-Cancer Drugs* **20:97–103 © 2009 Wolters Kluwer Health | Lippincott Williams & Wilkins.**

Anti-Cancer Drugs 2009, **20**:97–103

Keywords: FFC14A, KP1019, pharmacokinetics, phase I, ruthenium

[a]Department of Clinical Pharmacy, Institute of Pharmacy, University of Bonn, Bonn, [b]West German Cancer Centre, University of Essen, Essen, Germany, [c]Institute of Inorganic Chemistry, University of Vienna and [d]ACR-ITR Vienna and LBI-ACR Vienna, Kaiser Franz Josef-Spital, Vienna, Austria

Correspondence to Dr Ulrich Jaehde, PhD, Department of Clinical Pharmacy, Institute of Pharmacy, University of Bonn, An der Immenburg 4, Bonn 53121, Germany
Tel: +49 228 735252; e-mail: u.jaehde@uni-bonn.de

Received 14 September 2008 **Revised form accepted** 19 November 2008

Introduction

A novel anticancer ruthenium (III) complex (indazolium trans-[tetrachlorobis(1H-indazole)ruthenate(III)], KP1019, FFC14A, Fig. 1) has been developed to the stage of a first clinical trial [1]. After intravenous administration, KP1019 is highly bound to plasma proteins, mainly to albumin and to a smaller extent to transferrin as well [2–6].

The exact mechanism of action is not yet fully elucidated. Important steps are supposed to be the binding to transferrin through occupation of iron-binding sites and the transport into the cell via transferrin receptors [5–8]. On account of the high iron requirement of tumour cells resulting in the expression of a large number of transferrin receptors, a specific accumulation of ruthenium (III) complexes in tumour cells has been assumed [5–7,9]. Intracellularly, the ruthenium (III) species is released from transferrin and reduced to ruthenium (II) [10–12]. Owing to the hypoxic and thus slightly acidic conditions in solid tumours, this reduction is supposed to be enhanced in tumour tissue [13,14]. Cell death is thought to be caused by induction of apoptosis through the mitochondrial pathway by depolarisation of mitochondrial membranes (interference with mitochondrial electron transport chain), downmodulation of endogenous bcl-2 and activation of caspase-3 [15]. Preclinical data revealed promising activity against several types of tumours [15–22].

Recently, a clinical phase I trial was conducted in patients suffering from different types of solid tumours [1,23]. Five of six evaluable patients showed stable disease [23]. Here we report the pharmacokinetic analysis of ruthenium in this phase I trial and discuss the relevance of protein binding.

The aim of this study was to characterise the pharmacokinetic disposition of KP1019 in humans, for the first time. Moreover, the study was conducted to develop a pharmacokinetic model to support the development of rational dosing regimens in phase II studies.

Patients and methods

Patients

Blood sampling was performed within a two-center dose-escalating phase I study which was conducted to investigate the safety and pharmacokinetics of KP1019. Patients were recruited at the Kaiser Franz Josef Spital, Vienna, Austria, and at the West German Cancer Center, University of Essen, Germany. The study protocol was approved by the local ethics committees. All procedures were in accordance with the Helsinki declaration of 1975 (as revised in 2000).

Female and male patients aged above 18 years with histologically and cytologically confirmed advanced solid tumours refractory to standard therapy or for whom

0959-4973 © 2009 Wolters Kluwer Health | Lippincott Williams & Wilkins DOI: 10.1097/CAD.0b013e328322fbc5

Copyright © Lippincott Williams & Wilkins. Unauthorized reproduction of this article is prohibited.

Fig. 1

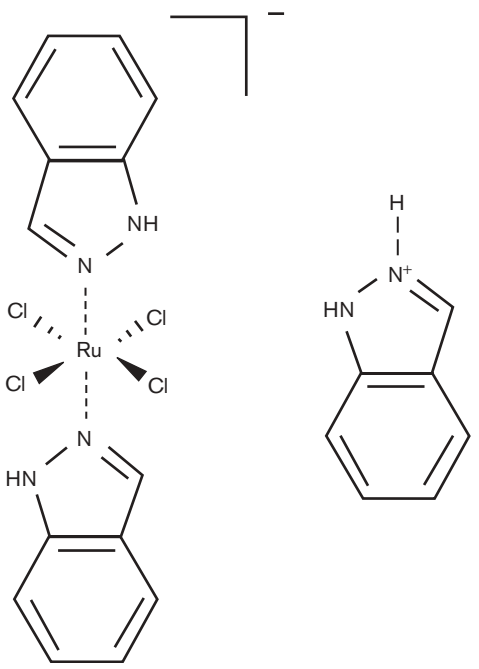

Chemical structure of KP1019 (FFC14A).

no established therapy existed were eligible. Their last cancer treatment (chemotherapy, hormone therapy, immune therapy, radiotherapy) had to be finished at least 4 weeks before study entry (in the case of extended radiotherapy or nitrosourea-containing chemotherapy the exclusion period was 6 weeks). The patients' performance status had to be ≤ 2 (The Measurement of Everyday Cognition scale) with a life expectancy of ≥ 3 months. Patients must have had normal hepatic and renal functions as confirmed by the following laboratory parameters: white blood cells $\geq 3.0 \times 10^9$/l, platelets $\geq 100 \times 10^9$/l, haemoglobin ≥ 10 g/dl, serum creatinine ≤ 1.4 mg/dl, creatinine clearance ≥ 60 ml/min, bilirubin ≤ 2.5 mg/dl, aspartate aminotransferase $\leq 2.5 \times$ upper limit of normal, alanine aminotransferase $\leq 2.5 \times$ upper limit of normal except for patients with liver metastases, where aspartate aminotransferase and alanine aminotransferase were allowed to be $5 \times$ the upper limit of normal.

Each of the following conditions represented an exclusion criterion: females who were pregnant or planned a pregnancy during the time of the trial, were nursing or were of childbearing potential and not using acceptable methods of contraception, patients with active infections, patients with poorly controlled coexisting medical conditions or severe malignant diseases which would be incompatible with the study protocol, patients with clinically verifiable disease of brain metastases or meningeal carcinosis, patients who were addicted to drugs or alcohol, patients with psychiatric or emotional problems, which would invalidate the informed consent or limit the ability of the patient to comply with the study requirements, patients who were unwilling or unable to provide the informed consent or to participate satisfactorily for the entire trial period. Written informed consent fulfilling the requirements of the ethics committee was required to be obtained from all patients before entry into the study.

Study design and treatment plan

KP1019 was administered intravenously twice weekly over 3 weeks (on days 1, 4, 8, 11, 15 and 18) at an infusion rate of 10 ml/min, starting at a total dose of 25 mg. The dosing schedule of two drug administrations per week alternating every third and fourth day was chosen because of the better feasibility in clinical practice as the drug could then be administered always on the same days of the week.

Dose escalation was performed according to an accelerated dose titration design with flat dose escalation of 100%. Toxicity was graded according to the National Cancer Institute Common Toxicity Criteria (NCI-CTC) version 2.0. The maximum tolerated dose was defined as the highest dose studied for which the incidence of dose-limiting toxicity was less than 33%. The dose-limiting toxicity was defined as any one of the following criteria: any NCI-CTC grade ≥ 3 nonhaematologic toxicity (excluding alopecia and nausea and vomiting sufficiently ameliorated by antiemetic treatment); NCI-CTC grade 4 complicated neutropenia (neutrophils $< 0.5 \times 10^9$/l and temperature > 38.5°C or clinical signs of infection); NCI-CTC grade 4 neutropenia lasting ≥ 7 days; NCI-CTC grade ≥ 3 thrombocytopenia ± haemorrhagic complications.

KP1019 (indazolium trans-[tetrachlorobis(1H-indazole) ruthenate(III)]) was reconstituted from the sodium salt and indazolium hydrochloride in a ratio of 1 : 1.1 according to the reaction:

$$Na[RuCl_4(Ind)_2] + 1.1\ HIndCl \rightarrow HInd\ [RuCl_4(Ind)_2] + NaCl + 0.1\ HIndCl$$

The trial drug was prepared right before the administration as follows: 50 mg sodium trans-[tetrachlorobis (1H-indazole)ruthenate(III)] were dissolved in exactly 13.33 ml isotonic salt solution and transferred to a sterile container. The total volume (117 ml) of a vial of indazole hydrochloride in a concentration of 0.145 mg/ml was added to the sterile container at room temperature. The prepared solution had to be clear and was administered through a sterile filter.

Sample collection

To investigate the pharmacokinetics of the ruthenium complex, plasma samples were collected before, during and after treatment. After the first and the fifth

Copyright © Lippincott Williams & Wilkins. Unauthorized reproduction of this article is prohibited.

administration, rich data sampling was performed with blood samples taken at the following time points: directly before infusion, at 20, 40 min and 1, 1.5, 2, 4, 8, 16, 20, 24, 32, 48 and 56 h after the end of the infusion. Additional blood samples were taken before each drug administration on days 4, 8, 11, 15 and 18 as well as 20, 40 and 60 min after drug administration on days 4 and 18. Urine was collected continuously after the first administration.

Determination of ruthenium in plasma and urine

The analysis of ruthenium in plasma and urine was performed by using a validated, element-specific graphite furnace atomic absorption spectrometry method. A SpectrAA Zeeman 220 atomic absorption spectrometer (Varian, Darmstadt, Germany) equipped with GTA 100 graphite tube atomizer (Varian) and a PSD 100 autosampler (Varian) was used. The graphite tubes were pyrolytically coated partition tubes.

The temperature programme was optimized for each matrix and concentration range. Working ranges comprised 30–60 000 µg/l Ru in plasma and 3–24 000 µg/l Ru in urine subdivided in three calibration ranges each. After a matrix-based calibration, plasma and urine samples were analysed after dilution with triton solution (1%) (Triton X-100, Sigma-Aldrich Chemie, Steinheim, Germany) or nitric acid (6.5%) (dilution of nitric acid 'Suprapur', 65% (V/V), Merck, Darmstadt, Germany). The temperature programmes are shown in Table 1. The lower limits of quantification were found to be 30 and 3 µg/l in plasma and urine, respectively. Both methods were fully validated and met the international requirements on bioanalytical methods [24,25].

Pharmacokinetic analysis

Individual pharmacokinetic parameters were estimated by using the validated software WinNonlin Professional Version 4.0 (Pharsight Corp., California, USA). Initial parameters for curve fitting were estimated using curve stripping based on plasma concentrations measured after the first administration. For evaluation of the complete concentration–time profiles, the final parameters estimated for the first administration were used as initial parameters after all administrations. For optimization of the model parameters the algorithm according to Gauss–Newton (modified by Levenberg and Hartley) was used. The concentrations were weighed using the weighing factor $1/\hat{C}_i^2$, with $\hat{C}_i$=model-predicted concentration at time i.

The following secondary pharmacokinetic parameters were calculated based on the model parameters: area under the curve extrapolated to infinity ($AUC_{0-\infty}$) for the first dose, total clearance (CL), volume of distribution at steady state (V_{ss}), half-life during the first elimination phase ($t_{1/2\ \lambda 1}$), and terminal half-life ($t_{1/2z}$).

Peak concentration (C_{max}) was directly taken from the respective concentration–time profile. Renal clearance (CL_R) was estimated in the intervals of continuous urine sampling ($CL_R(t_0–t_z)$) after the first administration. The AUC in the respective time interval ($AUC_{t0–tz}$) was calculated by the trapezoidal rule (with t_0=start of urine sampling, t_z=end of urine sampling interval). Renal clearance was then calculated according to the following equation:

$CL_R(t_0 - t_z) = \frac{U_{cum}(t_0 - t_z)}{AUC_{t_0 - t_z}}$ with U_{cum} (t_0–t_z) as cumulative amount of ruthenium in urine in the period t_0–t_z.

Total urinary excretion after the first dose was calculated as follows: $U_\infty(1^{st}\text{dose}) = CL_R(t_0 - t_z) \times AUC_\infty$ assuming $CL_R(t_0 - t_z) \sim CL_R(0 - \infty)$. The required AUC_∞ was taken from the compartmental data analysis of the plasma concentrations after the first administration. Moreover, urinary excretion was calculated as the percentage of the administered dose (U_∞[%1st dose]).

Statistical analysis

To test for dose proportionality, the power model was applied [26]. Therefore, the natural logarithms of the AUC values were linearly related to the natural logarithm of the dose according to the following formula:

$$\ln(\text{AUC}) = \beta_0 + \beta_1 \times \ln(\text{dose})$$

Table 1 **Temperature programme settings**

	Plasma				Urine		
Phase	Temperature (°C)	Time (s)	Gas flow (l/min)	Phase	Temperature (°C)	Time (s)	Gas flow (l/min)
Drying	95	5.0	3.0	Drying	95	5.0	3.0
	110	60.0	3.0		110	60.0	3.0
	120	10.0	3.0		120	10.0	3.0
Preashing	650	15.0	3.0	Preashing	650	15.0	3.0
	650	20.0	3.0		650	20.0	3.0
Ashing	1500	10.0	3.0	Ashing	1600	10.0	3.0
	1500	20.0	3.0		1600	20.0	3.0
	1500	2.0	0.0		1600	2.0	0.0
Atomization	2700	0.7	0.0	Atomization	2700	0.7	0.0
	2700	2.0	0.0		2700	2.0	0.0
Cleaning	2700	2.0	3.0	Cleaning	2700	2.0	3.0

Copyright © Lippincott Williams & Wilkins. Unauthorized reproduction of this article is prohibited.

Dose proportionality was checked by the following formula:

$$1+\frac{\ln(\theta_L)}{\ln(r)}<\beta_1<1+\frac{\ln(\theta_H)}{\ln(r)}$$

with θ_L=0.80, θ_H=1.25 and r=maximal dose ratio (=highest dose/lowest dose).

Results

Seven patients were included in the study. Patient characteristics are shown in Table 2. Administered doses were 25–600 mg KP1019 equivalent to 5.0–120.8 mg of ruthenium. Patient 6 (600 mg) did not complete the study. Therefore, a second patient was recruited for the respective dose level. Infusion duration was 0.1–4.25 h dependent on the volume of drug solution administered. Dose escalation was terminated without having reached the maximum tolerated dose because of limited solubility of the compound requiring increasingly large infusion volumes. No dose-limiting toxicity was observed.

A representative concentration–time curve is shown in Fig. 2 (patient 5, dose: 400 mg KP1019). Plasma concentrations of ruthenium were best described by a two-compartment model. The pharmacokinetic parameters were calculated in two ways: first by using concentrations measured after the first dose only (Table 3) and second using all available concentrations of an individual patient (Table 4). Individual clearance values ranged between 0.42 and 1.29 ml/min, volumes of distribution at steady state between 3.96 and 10.5 l, and the terminal half-life between 51.2 and 290 h.

To evaluate whether the pharmacokinetics of ruthenium was dose linear, the AUC values were plotted against the dose (Fig. 3). The AUC values increased proportionally with dose. In addition, dose proportionality was tested with the power model. Calculated β_1 values were 0.96 and 1.00 using concentrations after the first administration only and all available concentrations, respectively, and ranged between the calculated limits of 0.93 and 1.07 indicating dose proportionality. Consequently, clearance and volume of distribution were rather constant over the dose range studied.

After the first administration cumulative urinary excretion extrapolated to infinity ranged between 0.79 and 5.20% of the administered dose. Calculated renal clearance was low with values between 8 and 46 µl/min (Table 3).

Table 2 Patient characteristics

Sex	
Male	4
Female	3
Age (years)	
Median	58
Range	38–76
Body weight (kg)	
Median	70
Range	52–93
Height (cm)	
Median	167
Range	164–178
Tumour type	
Colorectal	2
Bladder	1
Liver cholangiocellular	1
Endometrium	1
Melanoma	1
Tongue	1

Fig. 2

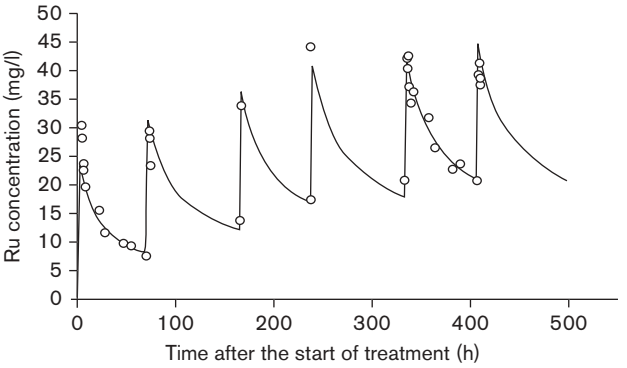

Ruthenium concentrations in plasma of patient 5 after six administrations of 400 mg KP1019. The circles depict the measured concentrations and the line represents the estimated concentrations according to the pharmacokinetic model.

Table 3 Pharmacokinetic parameters based on ruthenium concentrations after the first administration only

Patient	1	2	3	4	5	6	7
Dose KP1019 (mg)	25	50	100	200	400	600	600
C_{max} (mg/l)	1.26	1.96	4.46	10.8	30.5	29.0	24.9
$AUC_{0-\infty}$ (mgxh/l)	88.6	190	329	691	1442	2151	1566
$t_{1/2\ \lambda 1}$ (h)	4.28	5.21	6.09	6.86	1.59	2.50	3.38
$t_{1/2\ z}$ (h)	80.6	117	90.5	69.0	51.2	68.1	54.9
CL (ml/min)	0.95	0.88	1.02	0.97	0.93	0.94	1.29
V_{ss} (l)	6.41	8.67	7.63	5.46	3.96	5.43	6.00
CL_R (ml/min)	0.031	0.046	0.033	0.008	0.020	0.026	0.023
U_∞ (% of first dose)	3.23	5.20	3.23	0.79	2.15	2.75	1.79

AUC, area under the curve; C_{max}, peak concentration; CL, total clearance; V_{ss}, volume of distribution at steady state.

Table 4 Pharmacokinetic parameters based on all measured ruthenium concentrations

Patient	1	2	3	4	5	6	7
Dose KP1019 (mg)	25	50	100	200	400	600	600
C_{max} (mg/l)	2.63	4.67	7.96	22.5	43.0	ND	51.5
AUC (mg xh/l)	143	339	468	1605	2635	ND	4499
$t_{1/2\ \lambda 1}$ (h)	4.14	7.71	10.6	10.6	11.9	ND	17.6
$t_{1/2\ z}$ (h)	151	254	161	229	157	ND	290
CL (ml/min)	0.59	0.49	0.72	0.42	0.51	ND	0.45
V_{ss} (l)	7.46	10.5	9.37	7.83	6.32	ND	10.4

AUC, area under the curve; C_{max}, peak concentration; CL, total clearance; ND, not determined; V_{ss}, volume of distribution at steady state.

Copyright © Lippincott Williams & Wilkins. Unauthorized reproduction of this article is prohibited.

Fig. 3

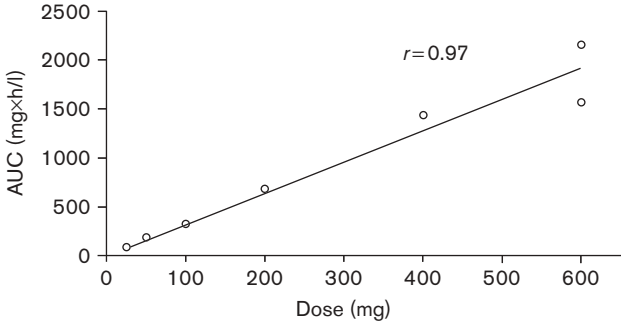

Correlation between ruthenium area under the curve (AUC) and dose after the first administration of KP1019.

Fig. 4

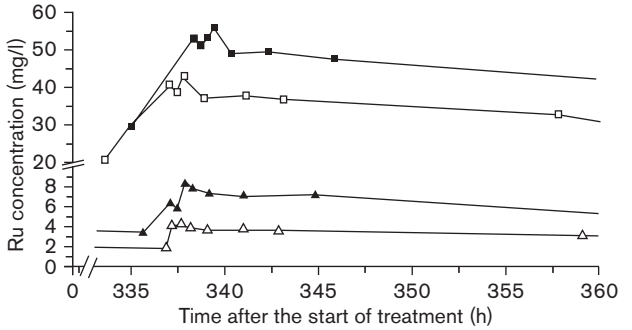

Ruthenium plasma concentrations versus time curve after the fifth administration of 50 mg KP1019 (patient 2, △), 100 mg KP1019 (patient 3, ▲), 400 mg KP1019 (patient 5, □) and 600 mg KP1019 (patient 7, ■).

In most of the concentration–time profiles a secondary peak or a plateau of the ruthenium concentrations was observed about 5–9 h after dosing. Two representative concentration–time curves are shown of two patients with low doses (patients 2 and 3 with doses of 50 and 100 mg KP1019, respectively; Fig. 4) and high doses (patients 5 and 7 with doses of 400 and 600 mg KP1019, respectively; Fig. 4) after the fifth administration.

Discussion

In this study, first human pharmacokinetic data of ruthenium after the administration of KP1019 were generated. Plasma concentrations of ruthenium were measured after the first administration and under multiple-dosing conditions. As the half-life of ruthenium was, as expected from preclinical data, very long (average terminal half-life about 100 h), after the fifth administration steady-state conditions were not reached. Therefore, real steady-state pharmacokinetics of ruthenium could not be evaluated.

Pharmacokinetic analysis revealed a low clearance, small volume of distribution and long half-life. The pharmacokinetic disposition of the ruthenium complex is in accordance with the expected high protein binding to plasma proteins, especially albumin and transferrin [2,3], indicating that ruthenium is mainly located in the blood compartment. Measurement of ultrafilterable plasma concentrations in individual samples of this study confirmed a low unbound fraction of less than 1% (data not shown). These findings are in accordance with the hypothesis of specific ruthenium uptake into the tumour cells through transferrin receptors [7,9] and thus low toxicity as only the unbound fraction is considered to contribute to potential toxic effects.

Recently, both capillary electrophoretic and chromatographic methods were coupled to an element-specific inductively coupled plasma mass spectrometry detector for determining the distribution of Ru between serum proteins in human plasma samples taken from a patient participating in this phase I trial (treated with 600 mg KP1019). As observed in incubation studies, rapid binding of the compound to human serum proteins was shown, with a vast majority of the Ru being attached to human serum albumin (HSA) [27]. Both methods delivered essentially similar results within the standard deviations, and the molar ratios of Ru per HSA molecule were found to increase with the number of infusions to about 1.5 (Table 5). Only a minor amount of the ruthenium, approximately 1%, was found attached to human serum transferrin, probably because of the quick turnover of the transferrin cycle. The loading of the protein, however, was found to have a significant influence on the cellular uptake of the drug, in particular 'overloading' of transferrin was found to decrease the amount of Ru in the cell [28]. Taking into account that the concentration of transferrin is about 5% of the HSA concentration, a certain degree of Ru is estimated to be bound to transferrin (approximately every third transferrin molecule is estimated to be ruthenated; Table 6), but it is assured that transferrin is not overloaded and therefore can exhibit its antitumour activity, as observed in an in-vitro study [28].

Renal excretion of ruthenium was very low, indicated by the low fraction of the administered dose found in the urine and by the very low renal clearance. Thus, the route of renal excretion contributes only to a minor part for the elimination of ruthenium.

In nearly all patients, a secondary peak or a plateau in the concentration–time profile was detected with concentrations slightly increasing after about 5 to 9 h after the start of infusion. This might indicate that the compound is excreted into the bile and subsequently undergoes

Copyright © Lippincott Williams & Wilkins. Unauthorized reproduction of this article is prohibited.

Table 5 Molar ratio of Ru per HSA molecule in dependence of the sampling time and the analysis method

Infusion			Molar ratio KP1019/HSA	
No.	Time (day)	Sampling time (h)	CE-ICP-MS	SEC/IC-ICP-MS
1	1	24 h after 1st infusion	0.47 ± 0.06	0.37 ± 0.07
		48 h after 1st infusion	0.33 ± 0.02	0.29 ± 0.06
2	3	After 2nd infusion	0.91 ± 0.14	0.88 ± 0.18
3	7	After 3rd infusion	1.16 ± 0.09	1.05 ± 0.21
4	10	After 4th infusion	1.33 ± 0.10	1.14 ± 0.23
5	15	After 5th infusion	1.40 ± 0.10	1.19 ± 0.24
		24 h after 5th infusion	1.16 ± 0.10	0.93 ± 0.19
		48 h after 5th infusion	0.94 ± 0.03	0.81 ± 0.16
6	17	After 6th infusion	1.62 ± 0.15	1.40 ± 0.28

HSA, human serum albumin.

Table 6 Estimation of the amount of a transferrin–Ru conjugate in human plasma (at the Ru peak concentration after the 6th infusion)

Protein	Blood concentration (mmol/l)	Ru per protein after 6th infusion
HSA	0.6	1.5
Transferrin	0.03	0.3

HSA, human serum albumin.

enterohepatic circulation. Thus, this finding might indicate a potential route of elimination of KP1019 or its metabolites.

Moreover, the pharmacokinetic data were analysed for dose proportionality. The proportional increase of AUC with rising doses after the first dose and after all administrations indicates linear pharmacokinetics, which may facilitate the further clinical development of KP1019. When only the concentrations measured after the first dose were used for parameter estimation, terminal half-life seems to be shorter and clearance higher compared with the evaluation of all concentrations. This observation, however, can be attributed to the limited observation period after the first dose because of the subsequent second dose. As pharmacokinetics seems to be linear, a time dependence during multiple dosing is unlikely as well. This, however, has to be confirmed by data measured after real single-dose and steady-state conditions.

Comparable pharmacokinetics has been described for another ruthenium complex in clinical trials, imidazolium trans-[tetrachloro (dimethyl sulfoxide) (imidazole) ruthenate (III)] (NAMI-A). The pharmacokinetic parameters found for this compound were in the same range as for KP1019 with a small volume of distribution (V_{ss} about 10 l), a low clearance (CL about 2.8 ml/min) and a long half-life ($t_{1/2}$ about 50 h). The complex was also highly bound to proteins (unbound fraction of 1.4–4.6%) and binding kinetic studies revealed very fast reactions [29]. Moreover, secondary peaks of ruthenium plasma concentrations were observed 8–12 h after dosing [30]. However, there are also differences between both ruthenium complexes. The linear relation between dose and the resulting AUC was stronger for KP1019 than for NAMI-A for which only a weak correlation was found. Cumulative urinary excretion after the administration of NAMI-A was higher (16%) than for KP1019 although it was not extrapolated to infinity as in our study.

The following considerations about a rational dosing regimen can be drawn from the presented data: regarding the half-life, a dosing interval of about every 3 or 4 days (72 and 96 h, respectively) seems reasonable, but real steady-state data are still required to be able to define a plausible dosing schedule. KP1019 can be administered safely at doses of up to 600 mg. Dose-limiting toxicity did not occur at these dose levels. Even higher doses might be safe and might lead to higher efficacy, although the protein loading should be kept in mind when further escalating the dose.

In conclusion, pharmacokinetic data analysis using ruthenium concentrations revealed linear pharmacokinetics of KP1019. Clearance of ruthenium was low, renal elimination accounts only for a low fraction of excreted ruthenium. As secondary peaks were observed in the concentration–time curves, biliary excretion might play a role in the overall elimination of ruthenium from plasma. Volume of distribution was small and ruthenium was highly bound to proteins. We developed a pharmacokinetic model that adequately describes the ruthenium plasma concentration–time profiles. Our model should be confirmed in a larger number of patients and refined with data generated at steady state.

Acknowledgements

We gratefully acknowledge the support of Dr Eberhard Scheuch during the development of the analytical method. This work was financially supported by Faustus Forschungs Compagnie, Leipzig, Germany.

References

1 Hartinger CG, Zorbas-Seifried S, Jakupec MA, Kynast B, Zorbas H, Keppler BK. From bench to bedside–preclinical and early clinical development of the anticancer agent indazolium trans-[tetrachlorobis (1H-indazole)ruthenate(III)] (KP1019 or FFC14A). *J Inorg Biochem* 2006; **100**:891–904.
2 Hartinger CG, Hann S, Koellensperger G, Sulyok M, Groessl M, Timerbaev AR, *et al.* Interactions of a novel ruthenium-based anticancer drug (KP1019 or FFC14a) with serum proteins–significance for the patient. *Int J Clin Pharmacol Ther* 2005; **43**:583–585.
3 Trynda-Lemiesz L, Karaczyn A, Keppler BK, Kozlowski H. Studies on the interactions between human serum albumin and trans-indazolium (bisindazole) tetrachlororuthenate (III). *J Inorg Biochem* 2000; **78**:341–346.
4 Allardyce CS, Dyson PJ. Ruthenium in medicine: current clinical uses and future prospects. *Platinum Metals Rev* 2001; **45**:62–69.
5 Clarke MJ. Ruthenium metallopharmaceuticals. *Coord Chem Rev* 2002; **232**:69–93.
6 Kostova I. Ruthenium complexes as anticancer agents. *Curr Med Chem* 2006; **13**:1085–1107.
7 Kratz F, Hartmann M, Keppler B, Messori L. The binding properties of two antitumor ruthenium (III) complexes to apotransferrin. *J Biol Chem* 1994; **269**:2581–2588.
8 Kratz F, Messori L. Spectral characterization of ruthenium (III) transferrin. *J Inorg Biochem* 1993; **49**:79–82.

Copyright © Lippincott Williams & Wilkins. Unauthorized reproduction of this article is prohibited.

9 Kratz F, Keppler BK, Hartmann M, Messori L, Berger MR. Comparison of the antiproliferative activity of two antitumor ruthenium (III) complexes with their apotransferrin and transferrin-bound forms in a human colon cancer cell line. *Met Based Drugs* 1996; **3**:15–24.

10 Sava G, Pacor S, Bregant F, Ceschia V. Metal complexes of ruthenium: a potential class of selective anticancer drugs. *Anticancer Res* 1991; **11**:1103–1107.

11 Kratz F, Mulinacci N, Messori L, Bertini I, Keppler BK. Kinetic, spectroscopic and LPLC studies of the interactions of antitumor ruthenium (III) complexes with serum proteins. In: Anastassopoulou J, Collery P, Etienne JC, Theophanides Th, editors. *Metal ions in biology and medicine*. Paris: John Libbey & Co Ltd; 1992. pp. 69–74.

12 Sava G, Pacor S, Bregant F, Ceschia V. Metal complexes of ruthenium in cancer chemotherapy. In: Collery P, Poirer LA, Manfait M, Etienne JC, editors. *Metal ions in biology and medicine*. Paris: John Libbey & Co Ltd; 1990. pp. 471–475.

13 Kung A, Pieper T, Wissiack R, Rosenberg E, Keppler BK. Hydrolysis of the tumor-inhibiting ruthenium(III) complexes HIm trans-[RuCl4(im)2] and HInd trans-[RuCl4(ind)2] investigated by means of HPCE and HPLC-MS. *J Biol Inorg Chem* 2001; **6**:292–299.

14 Schluga P, Hartinger CG, Egger A, Reisner E, Galanski M, Jakupec MA, Keppler BK. Redox behavior of tumor-inhibiting ruthenium (III) complexes and effects of physiological reductants on their binding to GMP. *Dalton Trans* 2006; 1796–1802.

15 Kapitza S, Pongratz M, Jakupec MA, Heffeter P, Berger W, Lackinger L, *et al*. Heterocyclic complexes of ruthenium (III) induce apoptosis in colorectal carcinoma cells. *J Cancer Res Clin Oncol* 2005; **131**:101–110.

16 Fruhauf S, Zeller WJ. New platinum, titanium, and ruthenium complexes with different patterns of DNA damage in rat ovarian tumor cells. *Cancer Res* 1991; **51**:2943–2948.

17 Aird RE, Cummings J, Ritchie AA, Muir M, Morris RE, Chen H, *et al*. In vitro and in vivo activity and cross resistance profiles of novel ruthenium (II) organometallic arene complexes in human ovarian cancer. *Br J Cancer* 2002; **86**:1652–1657.

18 Depenbrock H, Schmelcher S, Peter R, Keppler BK, Weirich G, Block T, *et al*. Preclinical activity of trans-indazolium [tetrachlorobisindazoleruthenate(III)] (NSC 666158; IndCR; KP 1019) against tumour colony-forming units and haematopoietic progenitor cells. *Eur J Cancer* 1997; **33**:2404–2410.

19 Gaiddon C, Jeannequin P, Bischoff P, Pfeffer M, Sirlin C, Loeffler JP. Ruthenium (II)-derived organometallic compounds induce cytostatic and cytotoxic effects on mammalian cancer cell lines through p53-dependent and p53-independent mechanisms. *J Pharmacol Exp Ther* 2005; **315**:1403–1411.

20 Galeano A, Berger MR, Keppler BK. Antitumor activity of some ruthenium derivatives in human colon cancer cell lines in vitro. *Arzneimittelforschung* 1992; **42**:821–824.

21 Kapitza S, Jakupec MA, Uhl M, Keppler BK, Marian B. The heterocyclic ruthenium (III) complex KP1019 (FFC14A) causes DNA damage and oxidative stress in colorectal tumor cells. *Cancer Lett* 2005; **226**:115–121.

22 Mazumder UK, Gupta M, Karki SS, Bhattacharya S, Rathinasamy S, Thangavel S. Synthesis, anticancer and antibacterial activity of some novel mononuclear Ru (II) complexes. *Chem Pharm Bull (Tokyo)* 2004; **52**: 178–185.

23 Dittrich C, Scheulen ME, Jaehde U, Kynast B, Gneist M, Richly H, *et al*. Phase I and pharmacokinetic study of sodium trans-[tetrachlorobis(1H-indazole)ruthenate(III)]/indazolehydrochloride (1:1.1) (FFC14A, KP1019) in patients with solid tumors-a study of the CESAR Central European Society for Anticancer Drug Research-EWIV. *AACR Meeting Abstracts* 2005; **2005**:110–111.

24 Gastl G, Berdel W, Edler L, Jaehde U, Port R, Mross K, *et al*. Standard Operating Procedure for Clinical Trials of the CESAR Central European Society for Anticancer Drug Research-EWIV: SOP 12 Validation of Bioanalytical Methods. *Onkologie* 2003; **26** (**suppl**):S52–S55.

25 US Department of Health and Human Services. Guidance for Industry: Bioanalytical Method Validation. 2001.

26 Smith BP, Vandenhende FR, DeSante KA, Farid NA, Welch PA, Callaghan JT, Forgue ST. Confidence interval criteria for assessment of dose proportionality. *Pharm Res* 2000; **17**:1278–1283.

27 Sulyok M, Hann S, Hartinger CG, Keppler BK, Stingeder G, Koellensperger G. Two dimensional separation schemes for investigation of the interaction of an anticancer ruthenium (III) compound with plasma proteins. *J Anal At Spectrom* 2005; **20**:856–863.

28 Pongratz M, Schluga P, Jakupec MA, Arion VB, Hartinger CG, Allmaier G, Keppler BK. Transferrin binding and transferrin-mediated cellular uptake of the ruthenium coordination compound KP1019, studied by means of AAS, ESI-MS and CD spectroscopy. *J Anal At Spectrom* 2004; **19**:46–51.

29 Groessl M, Reisner E, Hartinger CG, Eichinger R, Semenova O, Timerbaev AR, *et al*. Structure-activity relationships for NAMI-A-type complexes (HL)[trans-RuCl4L(S-dmso)ruthenate(III)] (L = imidazole, indazole, 1,2,4-triazole, 4-amino-1,2,4-triazole, and 1-methyl-1,2,4-triazole): aquation, redox properties, protein binding, and antiproliferative activity. *J Med Chem* 2007; **50**:2185–2193.

30 Rademaker-Lakhai JM, van den BD, Pluim D, Beijnen JH, Schellens JH. A Phase I and pharmacological study with imidazolium-trans-DMSO-imidazole-tetrachlororuthenate, a novel ruthenium anticancer agent. *Clin Cancer Res* 2004; **10**:3717–3727.

Copyright © Lippincott Williams & Wilkins. Unauthorized reproduction of this article is prohibited.